12-1-1990

# Device for dispersal of micrometer- and submicrometer-sized particles in vaccum

D. P. Sheehan
*University of San Diego*, dsheehan@sandiego.edu

M. Carillo
*University of San Diego*

W. Heidbrink
*University of California, Irvine*

# Device for dispersal of micrometer- and submicrometer-sized particles in vacuum

D. P. Sheehan and M. Carillo[a)]
*Department of Physics, University of San Diego, San Diego, California 92110*

W. Heidbrink
*Department of Physics, University of California, Irvine, California 92717*

(Received 25 July 1990; accepted for publication 27 August 1990)

A simple, versatile device for dispersing micrometer- and submicrometer-sized particles in vacuum is described. The source allows control of particle size ($0.5\ \mu m \leqslant l \leqslant 200\ \mu m$) and particle flux density up to roughly $10^7\ cm^{-2}\ s^{-1}$. Several types of microparticles were successfully dispersed.

## I. INTRODUCTION

Micrometer- and submicrometer-sized particles have broad applications to a variety of natural phenomena and technological processes. In nature, microparticles—fine dust swept up by wind from exposed soils, pollen, soot from forest fires, micro-organisms, meteoritic dust, and dust from volcanoes—act as condensation nuclei for cloud formation and precipitation.[1] Astrophysically, dusts are found in stellar atmospheres, stellar winds, planetary nebula, molecular clouds,[2,3] in planetary magnetospheres,[4] in the heliosphere, near comets,[5,6] and in planetary rings such as those around Jupiter, Saturn, and Uranus.[7] Reactions on dust surfaces dominate interstellar chemistry, and it is presumed dusty plasmas play central roles in the formation of stellar and planetary systems.[8]

Technologically, microparticles are common chemical catalysts and are vital to crystal growth. High-velocity, submicrometer dusts are being investigated as SDI weapons. Microparticles are of concern to the semiconductor industry since they may contaminate integrated circuits whose elements can be of comparable size to that of dust. Magnetohydrodynamic[9] and electrohydrodynamic[10] power generation utilize dusts to optimize energy output. Charged microparticles are produced in rocket exhaust and combustion processes, notably in rich hydrocarbon flames.[11] Industrial electrostatic precipitators rely upon corona charging of dusts and smoke and their subsequent extraction via electric fields.[12] A fine review of dusty phenomena is given by Sodha and Guha.[13]

Dust sources for vacuum have been pursued by several workers over the last 30 years, with mixed success. Workers have attempted to disperse microspheres, mineral dusts, and even pollen grains by various electrostatic, mechanical, and acoustic means.[14] Primary impediments appear to have been mechanically separating grains from one another and dealing with strong adhesion of grains to surfaces. Grains are often composed of compounds which exhibit strong van der Waal forces or even hydrogen bonding. Moreover, many dielectric dusts accumulate electrical charges which give rise to strong electrostatic attractions to oppositely charged grains or to image charges induced in nearby metal. Consequently, dusts may adhere to one another and to surfaces with strengths approaching those achieved by chemical bonds. To disperse dust, one must overcome strong forces. In gaseous environments, dust dispersal is relatively easy since one may utilize turbulent gas flows to disperse, isolate, and mechanically support grains. In vacuum or low-pressure environments, however, one must rely upon other means.

This paper describes a simple, versatile device for dispersing micrometer and submicrometer particles, dusts, and microspheres in a vacuum. This device allows control of particle size and flux density, each over several orders of magnitude, and it is effective for a wide variety of particle compositions. This device is also effective at normal air pressure and is expected to work in zero gravity environments as well. Note: The terms "microparticle," "grain," and "dust" will be used interchangeably in the text.

## II. APPARATUS

The dusting apparatus consists of a dusting-dispersing cell which is shaken at high frequency by a pneumatic driver (see Figs. 1 and 2). The dispersing cell (duster) consists of three aluminum cylindrical chambers, between which are clamped fine screens, and within which are contained the dust and small, fiber-coated spheres (Fig. 2). The duster is shaken by a powerful pneumatic driver, coupled to the duster by a steel rod, and isolated from the vacuum by a metal bellows (see Fig. 1). The micrometer- or submicrometer-sized particles begin in a reservoir (uppermost chamber of the duster) and are shaken, ground, and vibrated from chamber to chamber, through a series of increasingly fine screens, until they exit the bottommost screen in their final form.

Aluminum was chosen for the duster to reduce its inertial mass in order to facilitate shaking at high frequency. The capacity of each chamber is roughly 5 $cm^3$. Assuming the reservoir chamber is initially filled to one quarter capacity with 1-$\mu$m-sized dust particles, the total reservoir load is roughly $10^{12}$ particles. If the duster maintains an

[a)]Permanent address: TRW Electronics and Technology Div., Redondo Beach, CA 90278.

 0034-6748/90/123871-05$02.00  

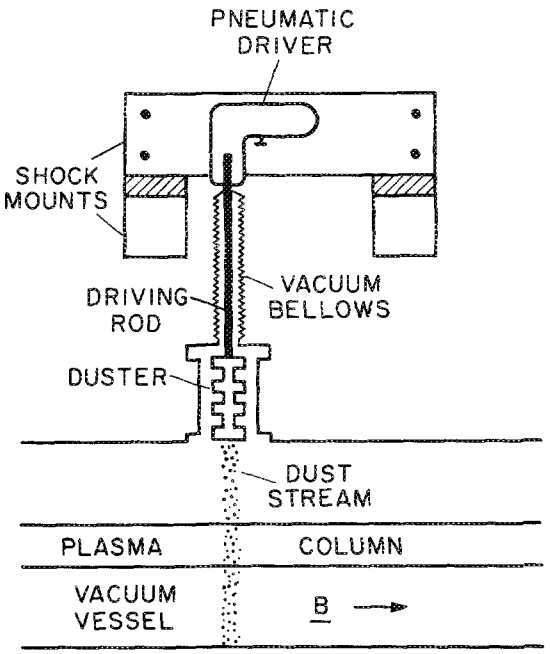


FIG. 1. Schematic of dusting device when mounted in UCI Q-machine.

output of $10^7$ particles/s, the initial load is adequate to maintain steady operation for roughly 15 h.

Fine screens [100 line per inch (lpi) to 2000 lpi; supplier: Buckbee-Mears), clamped between each chamber,

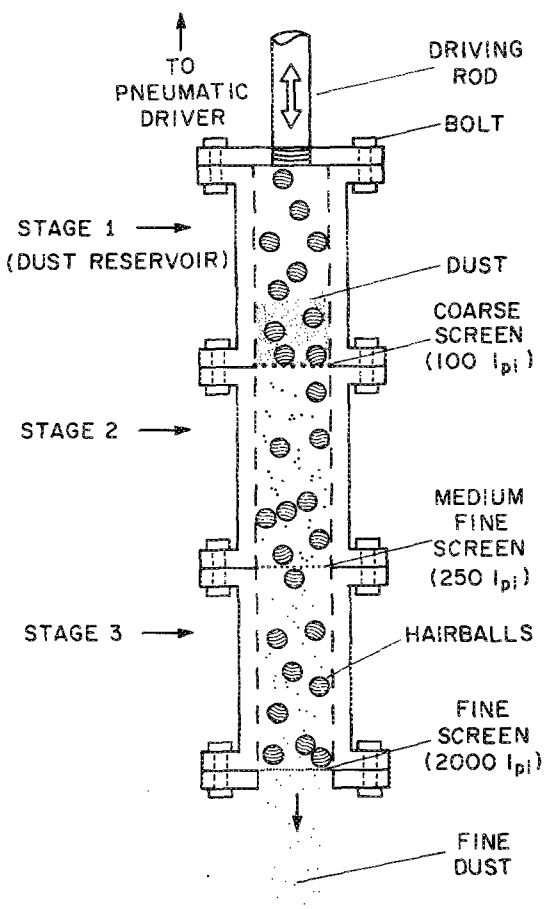


FIG. 2. Detail of dust chambers (duster).

help disperse the dust. Whereas van der Waals forces, hydrogen bonding, or electrostatic attraction between bare charges tend to clump dust particles, the dust's mechanical motion through the screen breaks and disperses it. The screen fineness is graduated from top to bottom with the coarsest screen between chambers 1 and 2, a medium grade screen between 2 and 3, and the finest screen at the bottom of chamber 3. Fine screens are fragile, and therefore were reinforced with a coarser, sturdier screen. The chambers are bolted together to allow easy changing of screen types. Lock washers are used to reduce the spontaneous disassembly of the duster caused by the violent shaking from the driver.

To illustrate one possible choice of screens, suppose the final particle size is desired to be less than 40 $\mu$m. One would fill stage 1, the reservoir, with dust whose individual grain size is less than or equal to 40 $\mu$m. The screens between stages 1 and 2 and stages 2 and 3 would be of fineness 100–250 lpi. This screen fineness would allow initial breakup of dust clumps, but also be sufficiently rugged to withstand pounding from the fiber-coated spheres within each chamber. The final screen at the bottom of stage 3 would be a 50% transparent 500-lpi screen, reinforced with a rugged 100-lpi screen facing the interior of the chamber. The upper size limit for dust exiting the duster is determined by the final stage's screen hole sizes. In fact, a spectrum of sizes is created, as will be discussed later. Assuming 50% transparency, the following screen finenesses are matched with their approximate upper limit of dust size: 100 lpi–180 $\mu$m, 250 lpi–70 $\mu$m, 500 lpi–35 $\mu$m, and 2000 lpi–10$\mu$m.

Each chamber houses approximately 10–20 small, fiber-coated, metal spheres ("hairballs"). These bounce violently within the chambers when the duster is shaken, thus grinding, milling, and agitating the dust. The core of a hairball consists of a small metal sphere 1–3 mm in diameter. A coat of fine fibers is attached to the sphere with a suitable adhesive. For our purposes, which involved high vacuum ($10^{-7}$ Torr) and strong magnetic fields (1–7 kG), pure copper shot (diamagnetic), low vapor-pressure epoxy, and virgin cotton fibers were employed.

The hairballs serve several roles. First, as the duster is driven, the balls grind and mill the dust. Many dusts, such as hydrated aluminum silicate (kaolin), are prone to clumping in large masses. The bouncing hairballs break the van der Waals and electrostatic bonds which bind the dust grains to one another. Second, the hairballs help agitate the dust through the screens where it otherwise tends to adhere. Dielectric dusts, if they carry electric charges, can adhere to metal screens, since they may induce image charges in the metal. Finally, by constantly impacting the screens, the hairballs prevent the screens from clogging with dust.

The fiber coating on a hairball serves as a macroscopic solvent onto which dust dissolves before it is freed by impact. The chemical composition and fineness of the fiber determines its effectiveness. For instance, while cotton fibers were found to be very effective for kaolin, human hair

and coarse synthetic rug fibers were not. Lint from a clothes dryer was found to be quite effective. The fibers also cushion the impact of the balls on the screens. It was found that unfibered metal spheres both damaged screens and tended to compact dust in the chambers.

Dusts were baked at elevated temperatures ($T \geqslant 400$ K) to drive off residual water. There was concern that the high surface area of the dust and fibers would result in unacceptable outgassing of the device in vacuum. This was not found to be the case.

The duster is shaken by a high-frequency, pneumatic driver (Campbell-Hausfeld Pneumatic Chiseler, Model 997897). The driver is powered by pressured $N_2$ (10–40 psi) from a standard laboratory tank. The driver produces a vertical linear motion at frequency $f = 5$–$80$ Hz with a linear displacement of 3–4 mm, depending on the gas pressure. The acceleration of the duster, hence the device's efficiency in dispersing dust, is sensitively dependent on many factors including the mechanical linkage of the duster to the driver, the $N_2$ pressure, the driver's spring constant, and the mass of the duster. Using a simple model, one may estimate the duster's acceleration. Let $y(t) = A \sin(\omega t)$ describe the vertical displacement of the duster, where $A$ is the maximum linear displacement from equilibrium and $\omega = 2\pi f$ is the driving frequency. For this experiment, let $A = 2$ mm and $\omega = 400$ rad/s. The duster's maximum acceleration, $a_{\max}$, is given by $a_{\max} = (d^2y/dt^2)_{\max} = -A\omega^2 \sim 300 \text{m/s}^2$, or about 30 g. Actually, the vertical displacement is nonsinusoidal, in which case the instantaneous acceleration of the duster can be much greater; the instantaneous accelerations of the duster may have been in excess of $10^3$ g. These large accelerations agitate the hairballs and help detach dust from the metallic screens.

The duster is linked to the pneumatic driver via a $\frac{1}{4}$-in.-diam 304 stainless-steel rod (Fig. 2). One end of the rod is bolted to the duster, incorporating a lock washer, and the other end inserted into the driver (chiseler) in place of its recommended chiseling tool. When operating in a vacuum, the rod is housed in a 30-cm-long mechanical bellows, its upper end vacuum sealed to the bellows. The bellows is rated for 20% compression and 50% extension of its overall length. Its actual excursion is small (3–4 mm), so that, even at high shaking frequencies, little metal fatigue occurs. The driver is mounted on a heavy wooden framework supplemented with styrofoam in order to minimize vibration to the vacuum system.

This device is effective both in vacuum and in gaseous atmospheres. It should also operate in zero-gravity environments as for dust experiments in space.

## III. RESULTS AND DISCUSSION

The dusting device successfully dispersed several types of micrometer- and submicrometer-sized particles in vacuum and at atmospheric pressures. Four screen types (50% transparent 100, 250, 500, and 2000 lpi) were investigated, as well as three dust types: (1) glass microspheres ($9.7 \pm 1.4$ $\mu$m), Duke Scientific Corp.; (2) graphite ($\sim 10$ $\mu$m); and (3) hydrated aluminum silicate, kaolin (0.1–4 $\mu$m) Sigma Chemical Co. The latter two dusts were chosen due to their similarity to those presumed to exist in interstellar space.[3]

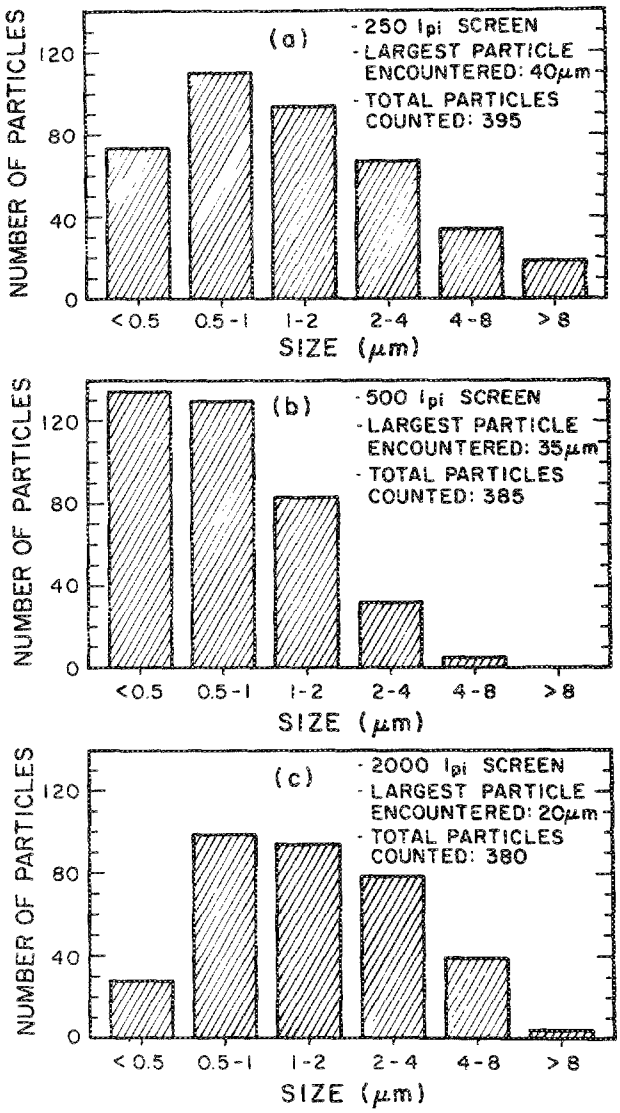


FIG. 3. Histogram of kaolin (0.1–0.4 $\mu$m) microparticles dispersed in vacuum by dusting apparatus with different screens on final stage of duster. (a) 250-lpi screen, (b) 500-lpi screen, and (c) 2000-lpi screen. Pneumatic driver operated at $f \sim 50$ Hz.

Figure 3 presents histograms of grain sizes for kaolin (0.1–4 $\mu$m) shaken through three different screen arrangements. The duster was configured with a 100- and 250-lpi screen below stages 1 and 2, respectively. The final screen, at the bottom of stage 3, was varied between 250, 500, and 2000 lpi. Analysis of dust was performed by Med-Tox Associates Inc., San Diego, using phase contrast microscopy. Dust samples were obtained by placing a clean microscope slide beneath the duster and subjecting it to a 0.1–0.2-s dose of dust. The driver was powered with 30-psi $N_2$ and operated at $f \sim 50$ Hz. Particle counts were established using random fields of view of the microscope. In every field,

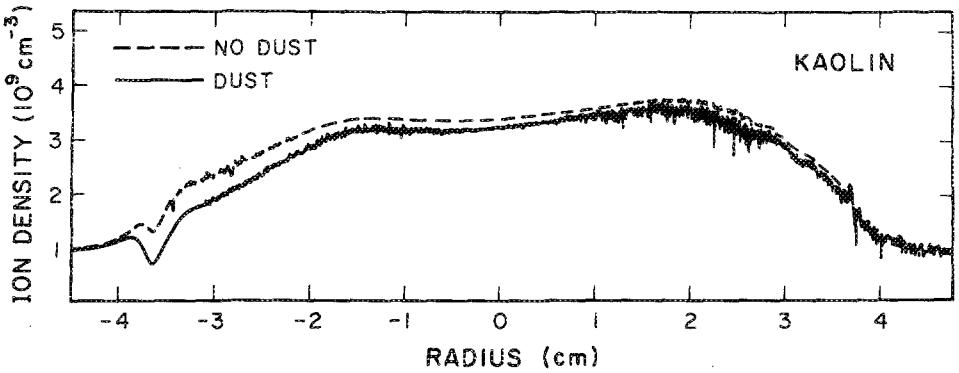


FIG. 4. Q-machine ion density profile in the direction perpendicular to plasma streaming and dust streaming vectors. Dotted line: dust absent from plasma. Solid line: kaolin dust present. Dust flux $I \sim 2\times10^7$ s$^{-1}$. Plasma parameters: $B = 1$ kG, $n \sim 4\times10^9$ cm$^{-3}$, $T_e \sim T_i \sim 0.2$ eV.

all particles were sized and assigned to one other six size groupings. In addition, the largest particle encountered on the slide was noted.

Figure 3 indicates different mesh screens produced different finenesses of dust. The coarsest screen, 250 lpi, produced the widest distribution of particle sizes, and the 500-lpi screen, the narrowest. It is not known why the 2000-lpi screen produced less fine particles less than the 500-lpi screen, but it is hypothesized that the proximity of the screen holes for the 2000-lpi screen allowed recombination of dust grains as they exited the screen.

The largest particle encountered was 40 $\mu$m for the 250-lpi screen, 35 $\mu$m for 500 lpi, and 20 $\mu$m for 2000 lpi. All screens produced over 85% of their final particle sizes in the range 0.1–0.4 $\mu$m, the size range asserted by their supplier, Sigma Chemical Co. The 500-lpi screen produced almost 99% of its particles within this range. In fact, all three screens configurations produced the majority of grains in the ($\leqslant$0.5 $\mu$m)–(2 $\mu$m) range. Note the lowest bin in the histogram ($\leqslant$0.5 $\mu$m) may underrepresent the true population of small grains, since phase contrast microscopy becomes less reliable for particles of size $\leqslant$0.5 $\mu$m.

For kaolin, monolayer dust coverage of a surface was achieved in roughly 5 s for all screens with the driver parameters identical with those above. The aperture on the bottom of the duster was roughly 1 cm$^2$. From this, assuming an average dust cross-sectional area of roughly 1 $\mu$m,[2] one infers that the duster delivered a particle flux density of roughly $10^7$ particles/cm$^2$ s. This agrees roughly with what one would expect for one grain falling from each microscopic hole in the screen per period of oscillation of the driver. The particle flux density may be varied by changing the agitation level of the duster.

Three types of dust were examined. Glass microphases and graphite grains passed through screens when subjected to small accelerations ($\sim$2 g). Hydrated aluminum silicate, kaolin, on the other hand, required large accelerations ($\sim$50 g) in order to be dispersed finely. At lower driving frequencies, kaolin clumped on the underside of screens and sloughed off in large masses, 0.1–1 mm in size. The differences in behavior between the various dust types, we believe, can be traced to their different predisposition to harbor excess electric charges, probably electrons.

## IV. APPLICATION

The parameter space for this dusting device includes a number of variables including screen size, driving frequency and amplitude, dust composition and grain size distribution, hairball size and number, fiber composition, and fineness. It appears these may be tailored to fit a wide variety of applications. In this section, the dusting device is applied to the investigation of dusty plasmas. Aluminum silicate (kaolin) and graphite were investigated since about half of interstellar dust is presumed to consist of amorphous silicates with the other half consisting of carbonaceous components such as graphite and amorphous carbon.[2]

A 1-cm$^2$-diam stream of kaolin (0.1–0.4 $\mu$m) with flux density $I \sim 2\times10^7$ grains/cm$^2$ s was injected perpendicularly across the center of a 5-cm-diam, Q-machine,[15] fully ionized, $Ba^+/e^-$ plasma column ($n_i = 4\times10^9$ cm$^{-3}$, $T_i = T_e = 0.2$ eV, $B = 1$ kG, $v_d \sim 1\times10^5$ cm/s) as shown in Fig. 1. Here $n$ is the plasma density, $T$ is temperature, $B$ is magnetic field strength, and $v_d$ is the plasma drift velocity. The plasma was created by contact ionization of barium atomic vapor on an incandescently-heated rhenium/tungsten disk (diameter 5 cm). The plasma drifted from the hot plate with velocity $v_d$, past the vertical dust stream, and terminated on a metallic, electrically floating cold plate roughly 1 m from the plasma source.

When kaolin dust was injected, a number of dust-plasma effects were noted including:

(1) alteration of the plasma column radial density profile;

(2) transport of dust along magnetic field lines;

(3) alterations of the plasma floating potential;

(4) increased low-frequency ($f \leqslant 20$ kHz) noise in the plasma;

(5) charging of dust grains (inferred from negative current flow to plates mounted below duster);

(6) alterations in standard Langmuir probe current/voltage traces; and

(7) depletion of plasma electron density.

These phenomena are planned to be discussed in length in a later communication. Figure 4 presents the radial ion density profile measured with a Langmuir probe 20 cm downstream of the duster in the presence of the dust

stream. The abscissa is the spatial coordinate perpendicular both to the plasma flow and dust flow. Notice that, in the presence of dust, the ion plasma density profile is depressed and noisier than in the dust's absence. The depletion of plasma density was accompanied by increased broadband, low-frequency turbulence ( $f \leqslant 20$ kHz). We hypothesize that the density loss may be due to degraded plasma confinement caused by this turbulence. Interestingly, low-frequency turbulence in cometary tails has been attributed to the presence of dust.[4] Future investigations may include studies of electron attachment and detachments from dust grains, transport in flowing plasmas, wave dispersion relations,[16] and studies of Coulomb solids.[17]

In summary, a simple, versatile device for the dispersal of micrometer- and submicrometer-sized particles has been described. A large range of particle compositions, sizes, and flux densities may be achieved in a controlled may be achieved in a controlled manner. A simple application of the duster to the study of dusty plasmas has been described.

## ACKNOWLEDGMENTS

It is a pleasure to thank Dr. Nathan Rynn for his support and to acknowledge the valuable technical assistance of David Parsons, Scott Keller, Mark Gladue, and Michael Zintl. These experiments were partially funded under NSF REU grant No. PHY-8803963, NSF grant No. PHY 8919331, and Research Corporation grant No. C-2953.

[1] H. G. Houghton, *Physical Meteorology* (MIT Press, Cambridge, MA, 1985).
[2] D. A. Mendis, Astrophys. Space Sci. **65**, 5 (1979).
[3] M. E. Bailey and D. A. Williams, Eds., *Dust in the Universe* (Cambridge University Press, Cambridge, 1988).
[4] D. A. Mendis, H. L. F. Houpis, and J. R. Hill, J. Geophys. Res. **87**, 3449 (1982).
[5] U. de Angelis, V. Formisano, and M. Giordano, J. Plasma Phys. **40**, 399 (1988).
[6] D. A. Mendis, J. R. Hill, H. L. F. Houpis, and E. C. Whipple, Jr., Astrophys. J. **249**, 787 (1981).
[7] C. K. Goertz, Rev. Geophys. **27**, 271 (1989).
[8] G. P. Horedt, Astrophys. Space Sci. **45**, 353 (1975).
[9] M. S. Sodha, C. J. Palumbo, and J. T. Daley, Brit. J. Appl. Phys. **14**, 916 (1963).
[10] J. Lawton, Brit. J. Appl. Phys. **15**, 935 (1964).
[11] H. Einbinder, J. Chem. Phys. **26**, 948 (1957).
[12] A. von Engel, *Ionized Gases* (Oxford University Press, Oxford, 1965), p. 254.
[13] M. S. Sodha and S. Guha, in *Advances in Plasma Physics*, edited by A. Simon and W. B. Thompson (Wiley, New York, 1971), Vol. 4.
[14] C. R. James and F. Vermeulen, Can. J. Phys. **46**, 855 (1968).
[15] N. Rynn, Rev. Sci. Instrum. **35**, 40 (1964).
[16] U. de Angelis, R. Bingham, and V. N. Tsytovich, J. Plasma Phys. **42**, 445 (1989).
[17] H. Ikezi, Phys. Fluids **29**, 1764 (1986).